

Coexistence of antiferromagnetic and ferromagnetic spin correlations in $\text{Ca}(\text{Fe}_{1-x}\text{Co}_x)_2\text{As}_2$ revealed by ^{75}As nuclear magnetic resonance

J. Cui,^{1,2} P. Wiecki,^{1,3} S. Ran*,^{1,3} S. L. Bud'ko,^{1,3} P. C. Canfield,^{1,3} and Y. Furukawa^{1,3}

¹*Ames Laboratory, U.S. DOE, Iowa State University, Ames, IA 50011, USA*

²*Department of Chemistry, Iowa State University, Ames, Iowa 50011, USA*

³*Department of Physics and Astronomy, Iowa State University, Ames, Iowa 50011, USA*

(Dated: August 23, 2016)

Recent nuclear magnetic resonance (NMR) measurements revealed the coexistence of stripe-type antiferromagnetic (AFM) and ferromagnetic (FM) spin correlations in both the hole- and electron-doped BaFe_2As_2 families of iron-pnictide superconductors by a Korringa ratio analysis. Motivated by the NMR work, we investigate the possible existence of FM fluctuations in another iron pnictide superconducting family, $\text{Ca}(\text{Fe}_{1-x}\text{Co}_x)_2\text{As}_2$. We re-analyzed our previously reported data in terms of the Korringa ratio and found clear evidence for the coexistence of stripe-type AFM and FM spin correlations in the electron-doped CaFe_2As_2 system. These NMR data indicate that FM fluctuations exist in general in iron-pnictide superconducting families and thus must be included to capture the phenomenology of the iron pnictides.

PACS numbers: 74.70.Xa, 76.60.-k, 75.50.Ee, 74.62.Dh

I. INTRODUCTION

Since the discovery of high T_c superconductivity in iron pnictides,¹ the interplay between spin fluctuations and the unconventional nature of superconductivity (SC) has been attracting much interest. In most of the Fe pnictide superconductors, the “parent” materials exhibit antiferromagnetic ordering below the Néel temperature.²⁻⁴ SC in these compounds emerges upon suppression of the stripe-type antiferromagnetic (AFM) phase by application of pressure and/or chemical substitution, where the AFM spin fluctuations are still strong. Therefore, it is believed that stripe-type AFM spin fluctuations play an important role in driving the SC in the iron-based superconductors, although orbital fluctuations are also pointed out to be important.⁵

Recently nuclear magnetic resonance (NMR) measurements revealed that ferromagnetic (FM) correlations also play an important role in both the hole- and electron-doped BaFe_2As_2 families of iron-pnictide superconductors.^{3,6,7} The FM fluctuations are found to be strongest in the maximally-doped BaCo_2As_2 and KFe_2As_2 , but are still present in the BaFe_2As_2 parent compound, consistent with its enhanced magnetic susceptibility χ .³ These FM fluctuations are suggested to compete with superconductivity and are a crucial ingredient to understand the variation of T_c and the shape of the SC dome.⁷ It is interesting and important to explore whether or not similar FM correlations exist in other iron pnictide systems.

The CaFe_2As_2 family has a phase diagram distinct from that for the BaFe_2As_2 family. Whereas for the BaFe_2As_2 materials the AFM and orthorhombic phase transitions become second order with Co substitution, the CaFe_2As_2 family continues to manifest a strongly first order, coupled, structural-magnetic phase transition even as Co substitution suppresses the transition

temperature to zero. Another significant difference in the phase diagrams of the CaFe_2As_2 and BaFe_2As_2 systems is also found in superconducting phase. Although SC appears when the stripe-type AFM phase is suppressed by Co substitution for Fe in both cases, no coexistence of SC and AFM has been observed in $\text{Ca}(\text{Fe}_{1-x}\text{Co}_x)_2\text{As}_2$, whereas the coexistence has been reported in $\text{Ba}(\text{Fe}_{1-x}\text{Co}_x)_2\text{As}_2$. These results are consistent with the difference between a strongly first order versus second order phase transition. Recent NMR measurements revealed that the stripe-type AFM fluctuations are strongly suppressed in the AFM state in the Co-doped CaFe_2As_2 system, whereas sizable stripe-type AFM spin fluctuations still remain in the AFM state in the Co-doped BaFe_2As_2 system.⁸ These results indicate that the residual AFM spin fluctuations play an important role for the coexistence of AFM and SC in $\text{Ba}(\text{Fe}_{1-x}\text{Co}_x)_2\text{As}_2$. Furthermore, in the case of $\text{Ca}(\text{Fe}_{1-x}\text{Co}_x)_2\text{As}_2$, pseudogap-like behavior⁸ has been observed in the temperature dependence of $1/T_1T$ and in-plane resistivity. The characteristic temperature of the pseudogap was reported to be nearly independent of Co substitution.

In this paper, we investigated the possible existence of FM fluctuations in $\text{Ca}(\text{Fe}_{1-x}\text{Co}_x)_2\text{As}_2$ and found the clear evidence of coexistence of stripe-type AFM and FM correlations based on ^{75}As NMR data analysis. In contrast to the case of $\text{Ba}(\text{Fe}_{1-x}\text{Co}_x)_2\text{As}_2$ where the relative strength of FM correlations increases with Co substitution, that of the FM correlations are almost independent of the Co content in $\text{Ca}(\text{Fe}_{1-x}\text{Co}_x)_2\text{As}_2$ from $x = 0$ to 0.059. Although we have investigated a relatively small Co substitution region, the existence of the FM spin correlations would be consistent with the fact that CaCo_2As_2 , the end member of the electron doped $\text{Ca}(\text{Fe}_{1-x}\text{Co}_x)_2\text{As}_2$ family of compounds, has an A-type antiferromagnetic ordered state below $T_N = 52\text{--}76\text{ K}$ ^{9,10} where the Co moments within the CoAs layer are ferro-

magnetically aligned along the c axis and the moments in adjacent layers are aligned antiferromagnetically. Since the coexistence of FM and AFM spin correlations are observed in both the hole- and electron-doped BaFe_2As_2 systems,⁷ our results suggest that the FM fluctuations exist in general in iron pnictide superconductors, indicating that theoretical microscopic models should include FM correlations to reveal the feature of the iron pnictides.

II. EXPERIMENTAL

The single crystals of $\text{Ca}(\text{Fe}_{1-x}\text{Co}_x)_2\text{As}_2$ ($x = 0, 0.023, 0.028, 0.033$ and 0.059) used in the present study are from the same batches as reported in Ref. 8. These single crystals were grown out of a FeAs/CoAs flux,^{11,12} using conventional high temperature growth techniques.^{13,14} Subsequent to growth, the single crystals were annealed at $T_a = 350$ °C for 7 days and then quenched. For $x = 0$, the single crystal was annealed at $T_a = 400$ °C for 24 hours. Details of the growth, annealing and quenching procedures have been reported in Refs. 11 and 12. The stripe-type AFM states have been reported below the Néel temperatures $T_N = 170, 106$, and 53 K for $x = 0, 0.023$, and 0.028 , respectively.¹⁵ The superconducting states are observed below the transition temperature of $T_c = 15$ and 10 K for $x = 0.033$ and 0.059 , respectively.¹²

NMR measurements were carried out on ^{75}As ($I = 3/2$, $\gamma/2\pi = 7.2919$ MHz/T, $Q = 0.29$ Barns) by using a lab-built, phase-coherent, spin-echo pulse spectrometer. The ^{75}As -NMR spectra were obtained at a fixed frequency $f = 53$ MHz by sweeping the magnetic field. The magnetic field was applied parallel to either the crystal c axis or the ab plane where the direction of the magnetic field within the ab plane was not controlled. The ^{75}As $1/T_1$ was measured with a recovery method using a single $\pi/2$ saturation rf pulse. Most of NMR experimental results were published elsewhere.^{8,16}

III. RESULTS AND DISCUSSION

In this paper we discuss magnetic correlations in $\text{Ca}(\text{Fe}_{1-x}\text{Co}_x)_2\text{As}_2$ based on a Korringa ratio analysis of the NMR results. Figure 1(a) shows the x and T dependence of the Knight shifts, K_{ab} for H parallel to the ab plane and K_c for H parallel to the c axis, where new Knight shift data for $x = 0.033$ and 0.059 are plotted in addition to the data ($x = 0, 0.023$ and 0.028) reported previously.^{8,16} The NMR shift consists of a T -independent orbital shift K_0 and a T -dependent spin shift $K_{\text{spin}}(T)$ due to the uniform magnetic spin susceptibility $\chi(\mathbf{q} = 0)$ of the electron system. The NMR shift can therefore be expressed as $K(T) = K_0 + K_{\text{spin}}(T) = K_0 + A_{\text{hf}}\chi_{\text{spin}}/N$, where N is Avogadro's number, and A_{hf} is the hyperfine coupling constant, usually expressed in units of T/μ_B . Since detailed analysis of the temperature dependence of K has been reported in Ref. 8,

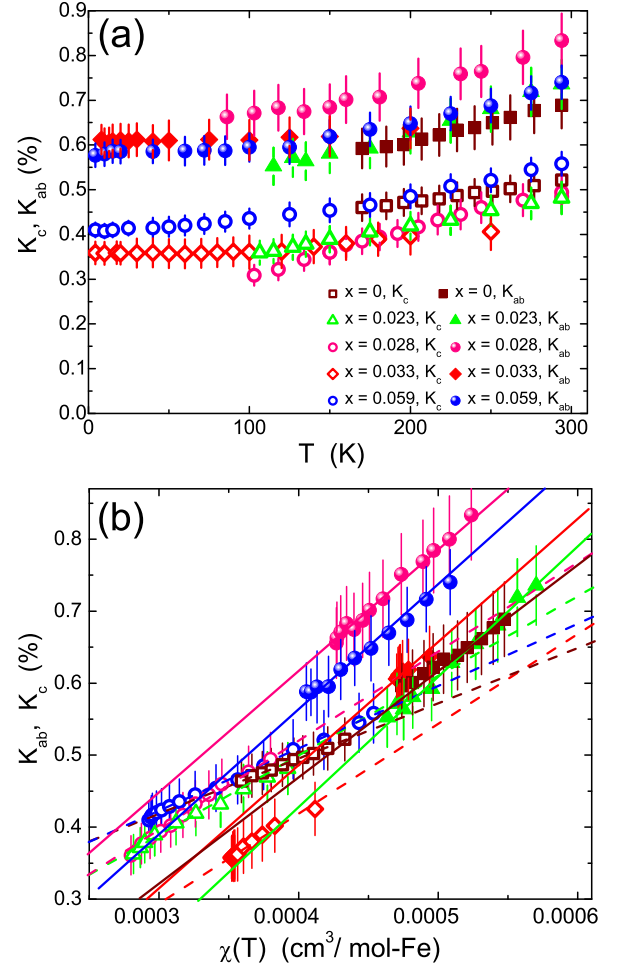


FIG. 1: (Color online) (a) Temperature dependence of ^{75}As NMR shifts K_{ab} and K_c for $\text{Ca}(\text{Fe}_{1-x}\text{Co}_x)_2\text{As}_2$. (b) $K(T)$ versus magnetic susceptibility $\chi(T)$ plots for the corresponding ab and c components of K in $\text{Ca}(\text{Fe}_{1-x}\text{Co}_x)_2\text{As}_2$ with T as an implicit parameter. The solid and broken lines are linear fits.

we are not going to discuss it in this paper. In order to extract $K_{\text{spin}}(T)$, which is needed for the following Korringa ratio analysis, we plot $K(T)$ against the corresponding bulk static uniform magnetic susceptibility $\chi(T)$ with T as an implicit parameter as shown in Fig. 1(b). From the slope of the linear fit curve, the hyperfine coupling constant can be estimated. The x dependence of the hyperfine coupling constant has been reported in Ref. 8. From the y -intercept of the linear fit curve, one can estimate the orbital shift K_0 , and extract $K_{\text{spin}}(T)$ to discuss magnetic correlations.

A Korringa ratio analysis is applied to extract the character of spin fluctuations in $\text{Ca}(\text{Fe}_{1-x}\text{Co}_x)_2\text{As}_2$ from ^{75}As NMR data as has been carried out for both the electron-doped $\text{Ba}(\text{Fe}_{1-x}\text{Co}_x)_2\text{As}_2$ and hole-doped $\text{Ba}_{1-x}\text{K}_x\text{Fe}_2\text{As}_2$ families of iron-pnictide SCs.⁷ Within a Fermi liquid picture, $1/T_1T$ is proportional to the square

of the density of states $\mathcal{D}(E_F)$ at the Fermi energy and $K_{\text{spin}} (\propto \chi_{\text{spin}})$ is proportional to $\mathcal{D}(E_F)$. In particular, $T_1 T K_{\text{spin}}^2 = \frac{\hbar}{4\pi k_B} \left(\frac{\gamma_e}{\gamma_N} \right)^2 = \mathcal{S}$, which is the Korringa relation. For the ^{75}As nucleus ($\gamma_N/2\pi = 7.2919 \text{ MHz/T}$), $\mathcal{S} = 8.97 \times 10^{-6} \text{ Ks}$. Korringa ratio $\alpha \equiv \mathcal{S}/(T_1 T K_{\text{spin}}^2)$, which reflects the deviations from \mathcal{S} , can reveal information about how electrons correlate in the material.^{17,18} $\alpha \sim 1$ represents the situation of uncorrelated electrons. On the other hand, $\alpha > 1$ indicates AFM correlations while $\alpha < 1$ for FM correlations. These come from the enhancement of $\chi(\mathbf{q} \neq 0)$, which increases $1/T_1 T$ but has little or no effect on K_{spin} , since the latter probes only the uniform $\chi(\mathbf{q} = 0)$. Therefore, the predominant feature of magnetic correlations, whether AFM or FM, can be determined by the Korringa ratio α .

To proceed with the Korringa ratio analysis, one needs to take the anisotropy of K_{spin} and $1/T_1 T$ into consideration. $1/T_1$ picks up the hyperfine field fluctuations at the NMR Larmor frequency, ω_0 , perpendicular to the applied field according to $(1/T_1)_{H||i} = \gamma_N^2 [|H_j^{\text{hf}}(\omega_0)|^2 + |H_k^{\text{hf}}(\omega_0)|^2]$, where (i, j, k) are mutually orthogonal directions and $|H_j^{\text{hf}}(\omega_0)|^2$ represents the power spectral density of the j -th component of the hyperfine magnetic field at the nuclear site. Thus, defining $H_{ab}^{\text{hf}} \equiv H_a^{\text{hf}} = H_b^{\text{hf}}$, which is appropriate for the tetragonal PM state, we have $(1/T_1)_{H||c} = 2\gamma_N^2 |H_{ab}^{\text{hf}}(\omega_0)|^2 \equiv 1/T_{1,\perp}$. The Korringa parameter $\alpha_{\perp} \equiv \mathcal{S}/T_{1,\perp} T K_{\text{spin},ab}^2$ will then characterize fluctuations in the ab -plane component of the hyperfine field. Similarly, we consider the quantity $1/T_{1,\parallel} \equiv 2(1/T_1)_{H||ab} - (1/T_1)_{H||c} = 2\gamma_N^2 |H_c^{\text{hf}}(\omega_N)|^2$, since $(1/T_1)_{H||ab} = \gamma_N^2 [|H_{ab}^{\text{hf}}(\omega_N)|^2 + |H_c^{\text{hf}}(\omega_N)|^2]$. We then pair $K_{\text{spin},c}$ with $1/T_{1,\parallel}$, so that the Korringa parameter $\alpha_{\parallel} = \mathcal{S}/T_{1,\parallel} T K_{\text{spin},c}^2$ characterizes fluctuations in the c -axis component of the hyperfine field.

Figure 2 shows the temperature dependence of $1/T_{1,\perp} T$ and $1/T_{1,\parallel} T$ in $\text{Ca}(\text{Fe}_{1-x}\text{Co}_x)_2\text{As}_2$ at $H \sim 7.5 \text{ T}$, obtained from the $(1/T_1 T)_{H||ab}$ and $(1/T_1 T)_{H||c}$ data reported previously.⁸ For $x = 0, 0.023$, and 0.028 , $1/T_{1,\parallel} T$ s show a monotonic increase with decreasing T down to $T_N = 170, 106$, and 53 K for $x = 0, 0.023, 0.028$, respectively, while $1/T_{1,\perp} T$ s are nearly independent of T although the slight increase can be seen near T_N for each sample. Since the increase of $1/T_{1,\parallel} T$ s originates from the growth of the stripe-type AFM spin fluctuations,⁸ the results indicate that the AFM spin fluctuations enhance the hyperfine fluctuations at the As sites along the c axis. In the case of superconducting samples with $x \geq 0.033$, $1/T_{1,\perp} T$ and $1/T_{1,\parallel} T$ show a slight increase or constant above $T^* \sim 100 \text{ K}$ on cooling and then start to decrease below T^* . These behaviors are ascribed to pseudogap-like behavior in Ref. 8. With a further decrease in T , both $1/T_{1,\parallel} T$ and $1/T_{1,\perp} T$ for $x = 0.033$ and 0.059 show sudden decreases below T_c [15 (10) K for $x = 0.033$ (0.059)] due to superconducting transitions.

Using the $1/T_{1,\perp} T$, $1/T_{1,\parallel} T$ data and Knight

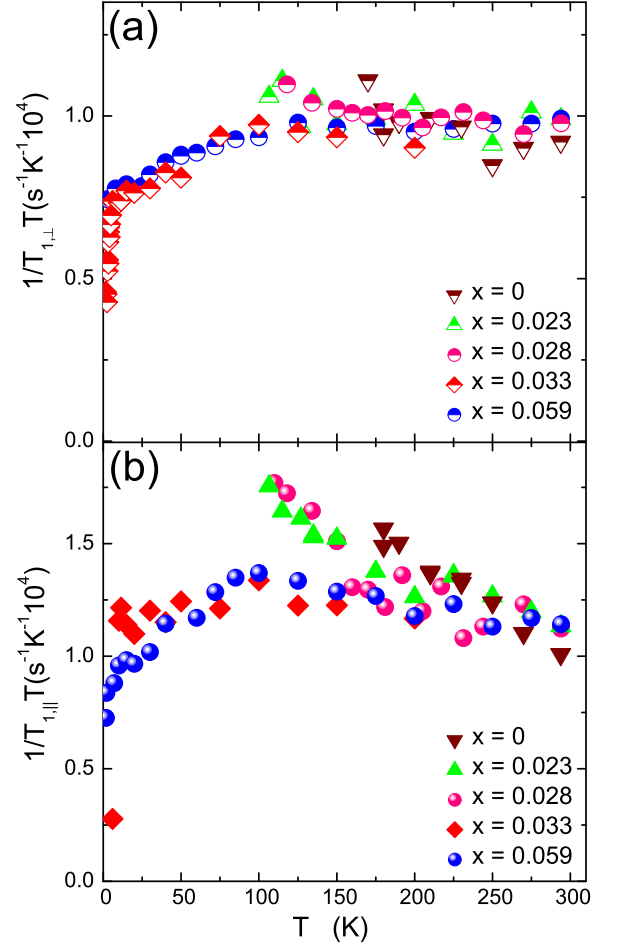


FIG. 2: (Color online) Temperature dependence of $1/T_1 T$ with anisotropy in $\text{Ca}(\text{Fe}_{1-x}\text{Co}_x)_2\text{As}_2$. (a) $1/T_{1,\perp} T = (1/T_1 T)_{H||c}$. (b) $1/T_{1,\parallel} T = 2(1/T_1 T)_{H||ab} - (1/T_1 T)_{H||c}$.

shift data, we discuss magnetic correlations in $\text{Ca}(\text{Fe}_{1-x}\text{Co}_x)_2\text{As}_2$ based on the Korringa ratios. The T dependences of the Korringa ratios $\alpha_{\perp} = \mathcal{S}/T_{1,\perp} T K_{\text{spin},ab}^2$ and $\alpha_{\parallel} = \mathcal{S}/T_{1,\parallel} T K_{\text{spin},c}^2$ are shown in Fig. 3(a). All α_{\parallel} and α_{\perp} increase with decreasing T down to T_N or T^* . The increase in α , which is the increase in $1/T_1 T K^2$, clearly indicates the growth of the stripe-type AFM spin correlations as have been pointed out previously.⁸ It is noted that α_{\parallel} is always greater than α_{\perp} for each sample, indicating that stronger hyperfine fluctuations at the As sites due to AFM correlations along the c axis than in ab . On the other hand, α_{\parallel} values seem to be less than unity: the largest value of α_{\perp} can be found to be ~ 0.4 in $x = 0$. The even smaller values α_{\perp} of $0.1 - 0.2$ in $x = 0.023$ and $x = 0.028$ at high temperatures are observed, suggesting FM fluctuations in the normal state.

In the application of the Korringa ratio to the iron pnictides, the question arises as to the role of the hyperfine form factor, which can, in principle, filter out the AFM fluctuations at the As site. This filtering effect

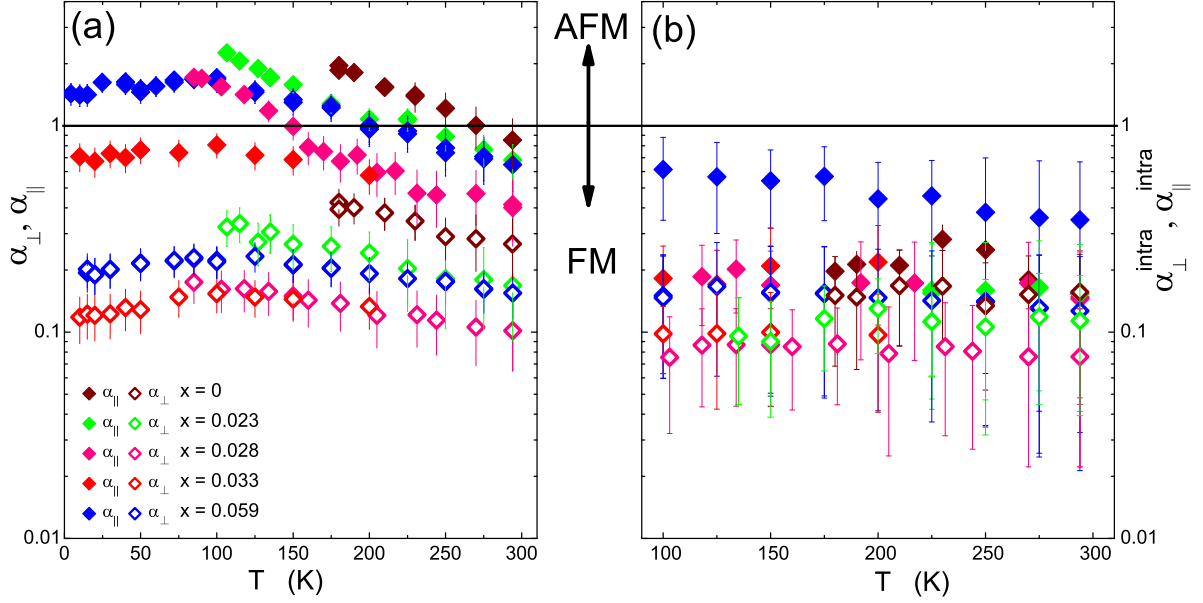


FIG. 3: (Color online) (a) T dependence of Korringa ratios, α_{\perp} and α_{\parallel} . (b) T dependence of intraband Korringa ratios, $\alpha_{\perp}^{\text{intra}}$ and $\alpha_{\parallel}^{\text{intra}}$, above T_N or T^* , obtained by subtracting a CW term from the temperature dependence of $1/T_{1,\perp}T$ and $1/T_{1,\parallel}T$ as described in the text.

could affect the balance of FM vs. AFM fluctuations as measured by the Korringa ratio.¹⁹ In order to discuss the filtering effects, it is convenient to express $1/T_1$ in terms of wave-number (\mathbf{q}) dependent form factors and \mathbf{q} dependent dynamical spin susceptibility $\chi(\mathbf{q}, \omega_0)$. By an explicit calculation of the form factors (see Appendix A) using the methods of Ref. 20, we find that

$$\frac{1}{T_{1,\parallel}T} \sim \left[\left(2.7 \frac{T^2}{\mu_B^2} \right) \frac{\chi''_{ab}(\mathbf{Q}, \omega_0)}{\hbar\omega_0} + \left(1.5 \frac{T^2}{\mu_B^2} \right) \frac{\chi''_c(\mathbf{0}, \omega_0)}{\hbar\omega_0} \right], \quad (1)$$

$$\frac{1}{T_{1,\perp}T} \sim \left[\left(3.2 \frac{T^2}{\mu_B^2} \right) \frac{\chi''_{ab}(\mathbf{0}, \omega_0)}{\hbar\omega_0} + \left(1.4 \frac{T^2}{\mu_B^2} \right) \frac{\chi''(\mathbf{Q}, \omega_0)}{\hbar\omega_0} \right] \quad (2)$$

where $\chi''(\mathbf{0}, \omega_0)$ and $\chi''(\mathbf{Q}, \omega_0)$ represent the imaginary part of the dynamical susceptibility for $\mathbf{q} = 0$ ferromagnetic and $\mathbf{Q} = (\pi, 0)/(0, \pi)$ stripe-type AFM components, respectively. The numbers are calculated from the hyperfine coupling constants in units of T/μ_B for CaFe_2As_2 given in Ref. 8. From these equations, it is clear that the stripe-type AFM fluctuations are not filtered out for both directions in the iron pnictides. It is also seen that for $1/T_{1,\parallel}T$, the form factor favors AFM fluctuations, which explains the larger (more AFM) values of α_{\parallel} . On the other hand, for $1/T_{1,\perp}T$, the ferromagnetic fluctuations dominate more than the AFM fluctuations as actually seen in Fig. 3(a) where α_{\perp} is less than α_{\parallel} for each sample.

Now we consider the origin of the hyperfine field at the ^{75}As site in order to further understand the physics associated with each term in Eqs. (1) and (2). The hyperfine field at the ^{75}As site is determined by the spin

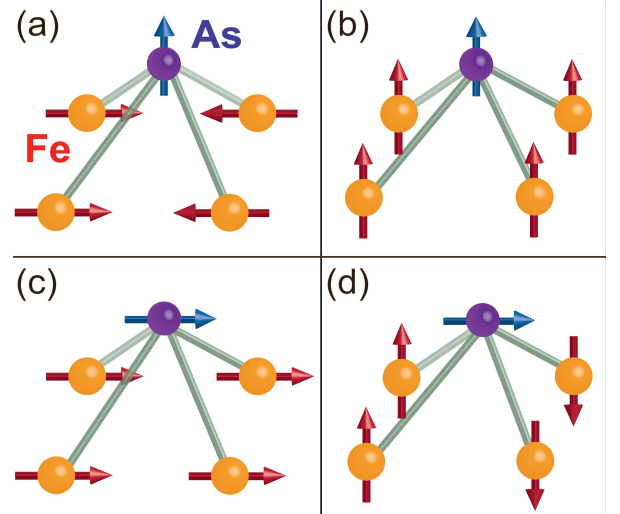


FIG. 4: (Color online) (a),(b): Sources of hyperfine field along the c -axis. (c),(d): Sources of hyperfine field in the ab -plane.

moments on the Fe sites through the hyperfine coupling tensor \tilde{A} , according to $\mathbf{H}^{\text{hf}} = \tilde{A} \cdot \mathbf{S}$. In the tetragonal PM phase, the most general form for \tilde{A} is^{21,22}

$$\tilde{A} = \begin{pmatrix} A_{\perp} & D & B \\ D & A_{\perp} & B \\ B & B & A_c \end{pmatrix}, \quad (3)$$

where A_i is the coupling for FM correlation, D is the coupling for in-plane Néel-type AFM correlation and B is coupling for stripe-type AFM correlations. Since there is

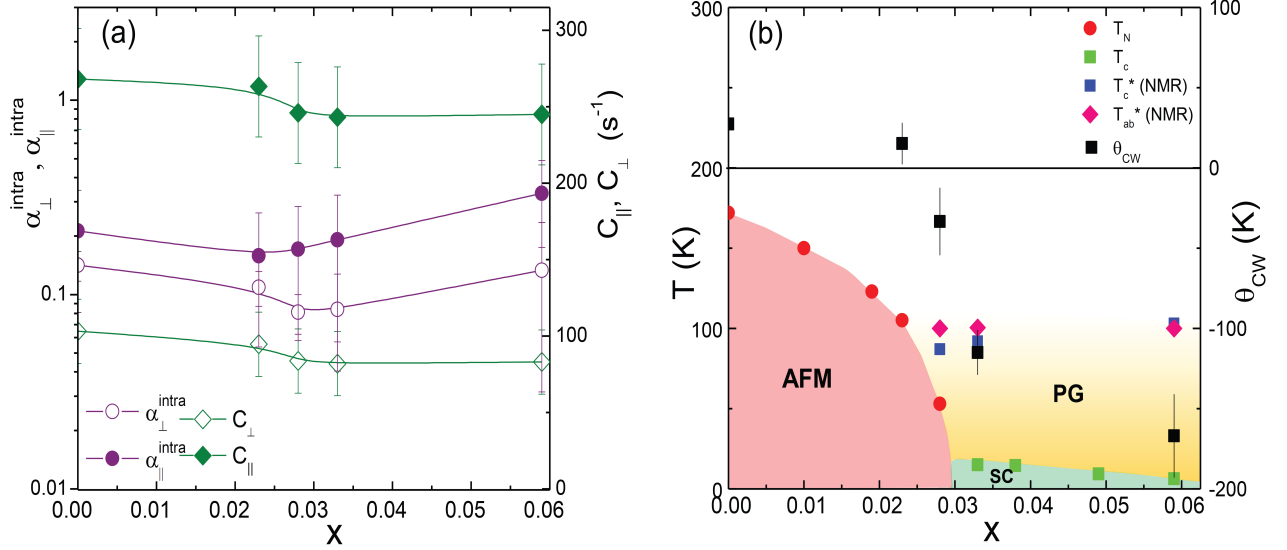


FIG. 5: (Color online) (a) Doping dependence of the T -independent values of $\alpha_{\perp}^{\text{intra}}$, $\alpha_{\parallel}^{\text{intra}}$ and Curie-Weiss parameters C_{\perp} , C_{\parallel} . The lines are guide for eyes. (b) Phase diagram of $\text{Ca}(\text{Fe}_{1-x}\text{Co}_x)_2\text{As}_2$. T_N and T_c are from Ref. 12. The pseudogap crossover temperature T_{ab}^* and T_c^* are determined by NMR measurements for $H \parallel ab$ plane and $H \parallel c$ axis, respectively. AFM, SC and PG stand for the antiferromagnetic ordered state, superconducting, and pseudogap phases, respectively.

no theoretical or experimental reason to expect Néel-type AFM correlation in the iron pnictides, below we simply set $D = 0$. We then obtain $H_{\perp}^{\text{hf}} = A_{\perp}S_{\perp} + BS_c$ and $H_c^{\text{hf}} = 2BS_{\perp} + A_cS_c$. There are therefore two sources of hyperfine field pointing along the c axis²¹: fluctuations at $\mathbf{q} = \mathbf{Q} = (\pi, 0)/(0, \pi)$ with the spins pointing in plane (as illustrated in Fig. 4(a)) or fluctuations at $\mathbf{q} = 0$ with the spins pointing along the c axis (Fig. 4(b)). The first and second fluctuations correspond to the first and second terms, respectively, in $1/T_{1,\parallel}T$ [Eq. (1)]. Similarly, hyperfine field fluctuations in the ab plane can result from fluctuations at $\mathbf{q} = 0$ with the spins pointing in plane (Fig. 4(c)), or from fluctuations at $\mathbf{q} = \mathbf{Q}$ with the spins pointing along the c axis (Fig. 4(d)). Again, the first and second fluctuations can be attributed to the first and second terms, respectively, in $1/T_{1,\perp}T$ [Eq. (2)]. In what follows, we will refer to the correlations depicted in Fig. 4(a) as “(a)-type” correlations (similarly for the others). To summarize, the value of α_{\parallel} reflects the competition between (a)- and (b)-type correlations, while α_{\perp} reflects the competition between (c)- and (d)-type correlations.

Now, since α_{\parallel} reflects the character of hyperfine field fluctuations with a c -axis component, the strongly AFM α_{\parallel} in Fig. 3 can be attributed to stripe-type AFM correlations with the Fe spins in plane (i.e. (a)-type). These must dominate the (b)-type correlations in order to have an AFM value of α_{\parallel} . Similarly, since α_{\perp} reflects the character of the ab -plane component of hyperfine field fluctuations, the strongly FM value of α_{\perp} in the high T region may be attributed to in plane FM fluctuations (Fig. 4(c)), while the increase of α_{\perp} as the temperature is lowered reflects the increasing dominance of stripe-type AFM correlations with a c -axis component to the spin

(as in Fig. 4(d)). By examining the c -axis and ab -plane components of the hyperfine field fluctuations separately via α_{\parallel} and α_{\perp} , we see the simultaneous coexistence of FM and AFM fluctuations in $\text{Ca}(\text{Fe}_{1-x}\text{Co}_x)_2\text{As}_2$. Furthermore, the dominance of (a)- and (c)-type spin fluctuations in the high temperature region suggests that both the AFM and FM fluctuations are highly anisotropic, favoring the ab -plane. A similar feature of the coexistence of FM and AFM fluctuations⁷ has been reported in $\text{Ba}(\text{Fe}_{1-x}\text{Co}_x)_2\text{As}_2$ and $\text{Ba}_{1-x}\text{K}_x\text{Fe}_2\text{As}_2$.

It is interesting to separate the FM and the stripe-type AFM fluctuations and extract their T dependence, as has been performed in the hole- and electron-doped BaFe_2As_2 .⁷ According to the previous paper,⁷ $1/T_1T$ was decomposed into inter- and intraband components according to $1/T_1T = (1/T_1T)_{\text{inter}} + (1/T_1T)_{\text{intra}}$, where the T dependence of the interband term is assumed to follow the Curie-Weiss (CW) form appropriate for 2D AFM spin fluctuations: $(1/T_1T)_{\text{inter}} = C/(T - \Theta_{\text{CW}})$. For T dependence of the intraband component, $(1/T_1T)_{\text{intra}}$ was assumed to be $(1/T_1T)_{\text{intra}} = \alpha + \beta \exp(-\Delta/k_B T)$. Here we also tried to decompose the present $1/T_{1,\parallel}T$ and $1/T_{1,\perp}T$ data following the procedure. We, however, found large uncertainty in decomposing our data, especially for the $1/T_{1,\perp}T$ case, due to the weak temperature dependence of $1/T_1T$. Nevertheless, we proceeded with our analysis to qualitatively examine the x dependence of Curie-Weiss parameter C , which measures the strength of AFM spin fluctuations, and Θ_{CW} corresponding to the distance in T from the AFM instability point. Here we fit the data above T_N or T^* for each sample. Θ_{CW} decreases from 38 ± 17 K ($x = 0$) to 15 ± 13 K ($x = 0.023$), and to a negative values of -33 ± 21 K ($x = 0.028$). This suggests

that compounds with $x = 0.023$ and 0.028 are close to the AFM instability point of $\Theta_{CW} = 0$ K. A similar behavior of Θ_{CW} is reported in $\text{Ba}(\text{Fe}_{1-x}\text{Co}_x)_2\text{As}_2$ (Refs. 7,23) and $\text{Ba}(\text{Fe}_{1-x}\text{Ni}_x)_2\text{As}_2$ (Ref. 24). The x dependences of CW parameters C_\perp , C_\parallel and Θ_{CW} are shown in Figs. 5(a) and (b) together with the phase diagram reported in Ref. 8. Although these parameters have large uncertainty, C_\parallel seems to be greater than C_\perp , consistent with that the in-plane AFM fluctuations are stronger than the c -axis AFM fluctuations. This result is same as in $\text{Ba}(\text{Fe}_{1-x}\text{Co}_x)_2\text{As}_2$ samples in Ref. 7. On the other hand, the C_\perp and C_\parallel parameters are almost independent of x in $\text{Ca}(\text{Fe}_{1-x}\text{Co}_x)_2\text{As}_2$ in the substitution range of $x = 0-0.059$, while the C_\perp and C_\parallel parameters decrease with Co substitution in BaFe_2As_2 where the c -axis component AFM spin fluctuations decrease and die out with $x \geq 0.15$.²³ It is interesting to point out that a similar x -independent behavior is also observed in the crossover temperature T^* attributed to the pseudogaplike behavior in the spin excitation spectra of $\text{Ca}(\text{Fe}_{1-x}\text{Co}_x)_2\text{As}_2$ system.⁸

Finally we show, in Fig. 3(b), the intra band Korringa ratios $\alpha_\parallel^{\text{intra}}$ and $\alpha_\perp^{\text{intra}}$ by subtracting the interband scattering term $C/(T - \Theta_{CW})$. Both $\alpha_\parallel^{\text{intra}}$ and $\alpha_\perp^{\text{intra}}$ remain roughly constant above T_N or T^* . We plotted the average value of $\alpha_\parallel^{\text{intra}}$ and $\alpha_\perp^{\text{intra}}$ as a function of x in Fig. 5(b). We find that $\alpha_\perp^{\text{intra}}$ is smaller than $\alpha_\parallel^{\text{intra}}$ for all the samples, confirming again the dominant in-plane FM spin fluctuations. The calculated $\alpha_\perp^{\text{intra}}$ and $\alpha_\parallel^{\text{intra}}$ in $\text{Ca}(\text{Fe}_{1-x}\text{Co}_x)_2\text{As}_2$ are almost same order with those in both the electron and hole doped BaFe_2As_2 . These results indicate that the FM spin correlations exist in general and may be a key ingredient to a theory of superconductivity in the iron pnictides.

IV. SUMMARY

Motivated by the recent NMR measurements which revealed the coexistence of the stripe-type antiferromagnetic (AFM) and ferromagnetic (FM) spin correlations in both the hole- and electron-doped BaFe_2As_2 families of iron-pnictide superconductors⁷, we have reanalyzed NMR data in $\text{Ca}(\text{Fe}_{1-x}\text{Co}_x)_2\text{As}_2$ and found clear evidence for the coexistence of the stripe-type AFM and FM spin correlations. In contrast to the case of $\text{Ba}(\text{Fe}_{1-x}\text{Co}_x)_2\text{As}_2$ where the relative strength of FM correlations increases with Co substitution, the FM correlations are almost independent of the Co substitution for our investigated range of $x = 0 - 0.059$ in $\text{Ca}(\text{Fe}_{1-x}\text{Co}_x)_2\text{As}_2$. The Curie-Weiss parameters $C_{\perp,\parallel}$ representing the strength of the stripe-type AFM correlations are almost independent of the Co doping, close to a feature of T^* representing a characteristic temperature of the pseudogaplike behavior. Our analysis of the NMR data indicates that FM fluctuations exist in general in iron-pnictide superconducting families. Further

systematic theoretical and experimental investigation on the role of the FM correlations in iron pnictide superconducting families are highly required.

V. ACKNOWLEDGMENTS

We thank David C. Johnston for helpful discussions. The research was supported by the U.S. Department of Energy, Office of Basic Energy Sciences, Division of Materials Sciences and Engineering. Ames Laboratory is operated for the U.S. Department of Energy by Iowa State University under Contract No. DE-AC02-07CH11358.

Appendix A: A calculation of form factor

Here, we directly calculate the appropriate form factors for the PM state of the iron pnictides according to the theory of Ref. 20. We make the assumption that the external applied field is much larger than the hyperfine field, which is certainly true in the PM state. We further assume that the wave-number q dependent dynamic susceptibility tensor $\chi^{\alpha\beta}(\mathbf{q}, \omega_0)$ is diagonal in the PM state. Under these assumptions, the spin-lattice relaxation rate in an external field \mathbf{h}_{ext} is given by

$$\frac{1}{T_1(\mathbf{h}_{\text{ext}})} = \lim_{\omega_0 \rightarrow 0} \frac{\gamma_N^2}{2N} k_B T \sum_{\alpha, \mathbf{q}} \mathcal{F}_{\alpha}^{\mathbf{h}_{\text{ext}}}(\mathbf{q}) \frac{\text{Im}[\chi^{\alpha\alpha}(\mathbf{q}, \omega_0)]}{\hbar\omega_0}, \quad (\text{A1})$$

where $\alpha = (a, b, c)$ sums over the crystallographic axes. The general expression for the q dependent form factor is

$$\mathcal{F}_{\alpha}^{\mathbf{h}_{\text{ext}}}(\mathbf{q}) = \sum_{\gamma, \delta} [R_{\mathbf{h}_{\text{ext}}}^{x\gamma} R_{\mathbf{h}_{\text{ext}}}^{x\delta} + (x \leftrightarrow y)] \mathcal{A}_{\mathbf{q}}^{\gamma\alpha} \mathcal{A}_{-\mathbf{q}}^{\delta\alpha}, \quad (\text{A2})$$

where $R_{\mathbf{h}_{\text{ext}}}$ is a matrix which rotates a vector from the crystallographic (a, b, c) coordinate system to a coordinate system (x, y, z) whose z axis is aligned with the total magnetic field at the nuclear site. For details we refer the reader to Ref. 20. When $\mathbf{h}_{\text{ext}} \parallel c$, the two coordinate systems coincide so that

$$R_{\mathbf{h}_{\text{ext}} \parallel c} = \begin{pmatrix} 1 & 0 & 0 \\ 0 & 1 & 0 \\ 0 & 0 & 1 \end{pmatrix}. \quad (\text{A3})$$

For $\mathbf{h}_{\text{ext}} \parallel a$, the appropriate matrix is

$$R_{\mathbf{h}_{\text{ext}} \parallel a} = \begin{pmatrix} 0 & 0 & 1 \\ 0 & 1 & 0 \\ -1 & 0 & 0 \end{pmatrix}. \quad (\text{A4})$$

For the case of the As site in the iron pnictides, the matrix $\mathcal{A}_{\mathbf{q}}$ in Eq. A2 is given by²⁰

$$\mathcal{A}_{\mathbf{q}} = 4 \begin{pmatrix} \mathcal{A}^{aa} c_a c_b & -\mathcal{A}^{ab} s_a s_b & i\mathcal{A}^{ac} s_a c_b \\ -\mathcal{A}^{ba} s_a s_b & \mathcal{A}^{bb} c_a c_b & i\mathcal{A}^{bc} c_a s_b \\ i\mathcal{A}^{ca} s_a c_b & i\mathcal{A}^{cb} c_a s_b & \mathcal{A}^{cc} c_a c_b \end{pmatrix}, \quad (\text{A5})$$

where $\mathcal{A}^{\alpha\beta}$ are the components of the hyperfine coupling tensor and

$$\begin{aligned} c_a &= \cos \frac{q_a a_0}{2} & c_b &= \cos \frac{q_b b_0}{2} \\ s_a &= \sin \frac{q_a a_0}{2} & s_b &= \sin \frac{q_b b_0}{2}. \end{aligned}$$

Here a_0 and b_0 are lattice constants. Of course, $a_0 = b_0$ in the PM state. Combining Eqs. A2-A5, we obtain

$$\mathcal{F}_a^{\mathbf{h}_{\text{ext}}\parallel a}(\mathbf{q}) = 16(\mathcal{A}^{ca}s_a c_b)^2 + 16(\mathcal{A}^{ba}s_a s_b)^2 \quad (\text{A6})$$

$$\mathcal{F}_b^{\mathbf{h}_{\text{ext}}\parallel a}(\mathbf{q}) = 16(\mathcal{A}^{cb}c_a s_b)^2 + 16(\mathcal{A}^{bb}c_a c_b)^2 \quad (\text{A7})$$

$$\mathcal{F}_c^{\mathbf{h}_{\text{ext}}\parallel a}(\mathbf{q}) = 16(\mathcal{A}^{cc}c_a c_b)^2 + 16(\mathcal{A}^{bc}c_a s_b)^2 \quad (\text{A8})$$

and

$$\mathcal{F}_a^{\mathbf{h}_{\text{ext}}\parallel c}(\mathbf{q}) = 16(\mathcal{A}^{aa}c_a c_b)^2 + 16(\mathcal{A}^{ba}s_a s_b)^2 \quad (\text{A9})$$

$$\mathcal{F}_b^{\mathbf{h}_{\text{ext}}\parallel c}(\mathbf{q}) = 16(\mathcal{A}^{bb}c_a c_b)^2 + 16(\mathcal{A}^{ab}s_a s_b)^2 \quad (\text{A10})$$

$$\mathcal{F}_c^{\mathbf{h}_{\text{ext}}\parallel c}(\mathbf{q}) = 16(\mathcal{A}^{ac}s_a c_b)^2 + 16(\mathcal{A}^{bc}c_a s_b)^2. \quad (\text{A11})$$

To calculate $1/T_1$ from Eq. A1, we assume for simplicity that $\chi^{\alpha\beta}(\mathbf{q}, \omega_0)$ is non-zero only near the wavevectors $\mathbf{q} = 0$, $\mathbf{q} = \mathbf{Q}_a \equiv (\pm\pi/a_0, 0)$ and $\mathbf{q} = \mathbf{Q}_b \equiv (0, \pm\pi/b_0)$. By tetragonal symmetry we have $a \leftrightarrow b$. In particular, $\mathbf{Q}_a = \mathbf{Q}_b \equiv \mathbf{Q}$ and $\text{Im}[\chi^{aa}(\mathbf{q}, \omega_0)] = \text{Im}[\chi^{bb}(\mathbf{q}, \omega_0)] \equiv \chi''_{ab}(\mathbf{Q}, \omega_0)$. We also now write $\text{Im}[\chi^{cc}(\mathbf{q}, \omega_0)] \equiv \chi''_c(\mathbf{Q}, \omega_0)$. We thus obtain

$$\begin{aligned} \frac{1}{T_1(\mathbf{h}_{\text{ext}}\parallel c)} &= \lim_{\omega_0 \rightarrow 0} \frac{8\gamma_N^2}{N} k_B T \left[2(\mathcal{A}^{aa})^2 \frac{\chi''_{ab}(\mathbf{0}, \omega_0)}{\hbar\omega_0} \right. \\ &\quad \left. + 4(\mathcal{A}^{ac})^2 \frac{\chi''_c(\mathbf{Q}, \omega_0)}{\hbar\omega_0} \right] \quad (\text{A12}) \end{aligned}$$

and

$$\begin{aligned} \frac{1}{T_1(\mathbf{h}_{\text{ext}}\parallel a)} &= \lim_{\omega_0 \rightarrow 0} \frac{8\gamma_N^2}{N} k_B T \left[4(\mathcal{A}^{ca})^2 \frac{\chi''_{ab}(\mathbf{Q}, \omega_0)}{\hbar\omega_0} \right. \\ &\quad + (\mathcal{A}^{aa})^2 \frac{\chi''_{ab}(\mathbf{0}, \omega_0)}{\hbar\omega_0} \\ &\quad + (\mathcal{A}^{cc})^2 \frac{\chi''_c(\mathbf{0}, \omega_0)}{\hbar\omega_0} \\ &\quad \left. + 2(\mathcal{A}^{ac})^2 \frac{\chi''_c(\mathbf{Q}, \omega_0)}{\hbar\omega_0} \right]. \quad (\text{A13}) \end{aligned}$$

We have summed over four AFM wavevectors $\mathbf{Q} = (\pm\pi/a_0, 0)$ and $\mathbf{Q} = (0, \pm\pi/a_0)$, which have the same value of $\chi''(\mathbf{Q}, \omega_0)$ in the PM state. Notice that, for both field directions, AFM fluctuations at $\mathbf{q} = \mathbf{Q}$ are completely filtered out if $\mathcal{A}^{ac} = 0$, as pointed out in Ref. 3. However, in the iron pnictides $\mathcal{A}^{ac} \neq 0$,²¹ and therefore AFM fluctuations are not filtered out. From Eqs. A12 and A13 we can easily calculate $1/T_{1,\parallel} \equiv 2/T_1(\mathbf{h}_{\text{ext}}\parallel a) - 1/T_1(\mathbf{h}_{\text{ext}}\parallel c)$ and $1/T_{1,\perp} \equiv 1/T_1(\mathbf{h}_{\text{ext}}\parallel c)$

$$\begin{aligned} \frac{1}{T_{1,\perp}} &= \lim_{\omega_0 \rightarrow 0} \frac{16\gamma_N^2}{N} k_B T \left[(\mathcal{A}^{aa})^2 \frac{\chi''_{ab}(\mathbf{0}, \omega_0)}{\hbar\omega_0} \right. \\ &\quad \left. + 2(\mathcal{A}^{ac})^2 \frac{\chi''_c(\mathbf{Q}, \omega_0)}{\hbar\omega_0} \right] \quad (\text{A14}) \end{aligned}$$

$$\begin{aligned} \frac{1}{T_{1,\parallel}} &= \lim_{\omega_0 \rightarrow 0} \frac{16\gamma_N^2}{N} k_B T \left[4(\mathcal{A}^{ca})^2 \frac{\chi''_{ab}(\mathbf{Q}, \omega_0)}{\hbar\omega_0} \right. \\ &\quad \left. + (\mathcal{A}^{cc})^2 \frac{\chi''_c(\mathbf{0}, \omega_0)}{\hbar\omega_0} \right] \quad (\text{A15}) \end{aligned}$$

Notice that the fluctuations probed by $1/T_{1,\parallel}$ and $1/T_{1,\perp}$ are consistent with the qualitative arguments used in the main text. For the case of CaFe_2As_2 , Ref. 8 gives $\mathcal{A}^{aa} = 1.8 \text{ T}/\mu_B$, $\mathcal{A}^{cc} = 1.2 \text{ T}/\mu_B$ and $\mathcal{A}^{ca} = \mathcal{A}^{ac} = 0.82 \text{ T}/\mu_B$. \mathcal{A}^{aa} and \mathcal{A}^{cc} are determined by Knight shift measurements and \mathcal{A}^{ac} is found by comparing the measured internal field in the AFM state to the value of the ordered moment obtained by neutron scattering.

* present address: Department of Physics, University of California, San Diego. California 92093, USA

-
- ¹ Y. Kamihara, T. Watanabe, M. Hirano, and H. Hosono, J. Am. Chem. Soc. **130**, 3296 (2008).
² P. C. Canfield and S. L. Bud'ko, Annu. Rev. Condens. Matter Phys. **1**, 27 (2010).
³ D. C. Johnston, Adv. Phys. **59**, 803 (2010).
⁴ G. R. Stewart, Rev. Mod. Phys. **83**, 1589 (2011).
⁵ Y. K. Kim, W. S. Jung, G. R. Han, K.-Y. Choi, C.-C. Chen, T. P. Devereaux, A. Chainani, J. Miyawaki, Y.

- Takata, Y. Tanaka, M. Oura, S. Shin, A. P. Singh, H. G. Lee, J.-Y. Kim, and C. Kim, Phys. Rev. Lett. **111**, 217001 (2013).
⁶ P. Wiecki, V. Ogloblichev, A. Pandey, D. C. Johnston, and Y. Furukawa, Phys. Rev. B **91**, 220406 (R) (2015).
⁷ P. Wiecki, B. Roy, D. C. Johnston, S. L. Budko, P. C. Canfield, and Y. Furukawa, Phys. Rev. Lett. **115**, 137001 (2015).

- ⁸ J. Cui, B. Roy, M. A. Tanatar, S. Ran, S. L. Bud'ko, R. Prozorov, P. C. Canfield, and Y. Furukawa, Phys. Rev. B **92**, 184504 (2015).
- ⁹ B. Cheng, B. F. Hu, R. H. Yuan, T. Dong, A. F. Fang, Z. G. Chen, G. Xu, Y. G. Shi, P. Zheng, J. L. Luo, and N. L. Wang, Phys. Rev. B **85**, 144426 (2012).
- ¹⁰ D. G. Quirinale, V. K. Anand, M. G. Kim, Abhishek Pandey, A. Huq, P. W. Stephens, T. W. Heitmann, A. Kreyssig, R. J. McQueeney, D. C. Johnston, and A. I. Goldman, Phys. Rev. B **88**, 174420 (2013).
- ¹¹ S. Ran, S. L. Bud'ko, D. K. Pratt, A. Kreyssig, M. G. Kim, M. J. Kramer, D. H. Ryan, W. N. Rowan-Weetaluktuk, Y. Furukawa, B. Roy, A. I. Goldman, and P. C. Canfield, Phys. Rev. B **83**, 144517 (2011).
- ¹² S. Ran, S. L. Bud'ko, W. E. Straszheim, J. Soh, M. G. Kim, A. Kreyssig, A. I. Goldman, and P. C. Canfield, Phys. Rev. B **85**, 224528 (2012).
- ¹³ P. C. Canfield, in *Properties and applications of complex intermetallics*, edited by E. Belin-Fr   (World Scientific Co. Pte. Ltd, Singapore, 2010), page 93.
- ¹⁴ P. C. Canfield and Z. Fisk, Philos. Mag. B **65**, 1117 (1992).
- ¹⁵ A. I. Goldman, D.N. Argyriou, B. Ouladdiaf, T. Chatterji, A. Kreyssig, S. Nandi, N. Ni, S.L. Budko, P.C. Canfield, and R.J. McQueeney, Phys. Rev. B **78**, 100506(R) (2008).
- ¹⁶ Y. Furukawa, B. Roy, S. Ran, S. L. Bud'ko, and P. C. Canfield, Phys. Rev. B **89**, 121109 (2014).
- ¹⁷ T. Moriya, J. Phys. Soc. Jpn. **18**, 516 (1963).
- ¹⁸ A. Narath and H. T. Weaver, Phys. Rev. **175**, 373 (1968).
- ¹⁹ P. Jegli  , A. Poto  nik, M. Klanj  sek, M. Bobnar, M. Jagodi  , K. Koch, H. Rosner, S. Margadonna, B. Lv, A. M. Guloy, and D. Ar  on, Phys. Rev. B **81**, 140511(R) (2010).
- ²⁰ A. Smerald and N. Shannon, Phys. Rev. B **84**, 184437 (2011).
- ²¹ K. Kitagawa, N. Katayama, K. Ohgushi, M. Yoshida, and M. Takigawa, J. Phys. Soc. Jpn. **77**, 114709 (2008).
- ²² M. Hirano, Y. Yamada, T. Saito, R. Nagashima, T. Konishi, T. Toriyama, Y. Ohta, H. Fukazawa, Y. Kohori, Y. Furukawa, K. Kihou, C-H Lee, A. Iyo and H. Eisaki, J. Phys. Soc. Jpn. **81**, 054704 (2012).
- ²³ F. L. Ning, K. Ahilan, T. Imai, A. S. Sefat, M. A. McGuire, B. C. Sales, D. Mandrus, P. Cheng, B. Shen, and H.-H. Wen, Phys. Rev. Lett. **104**, 037001 (2010).
- ²⁴ R. Zhou, Z. Li, J. Yang, D. L. Sun, C. T. Lin, and G.-q. Zheng, Nat. Commun. **4** (2013).